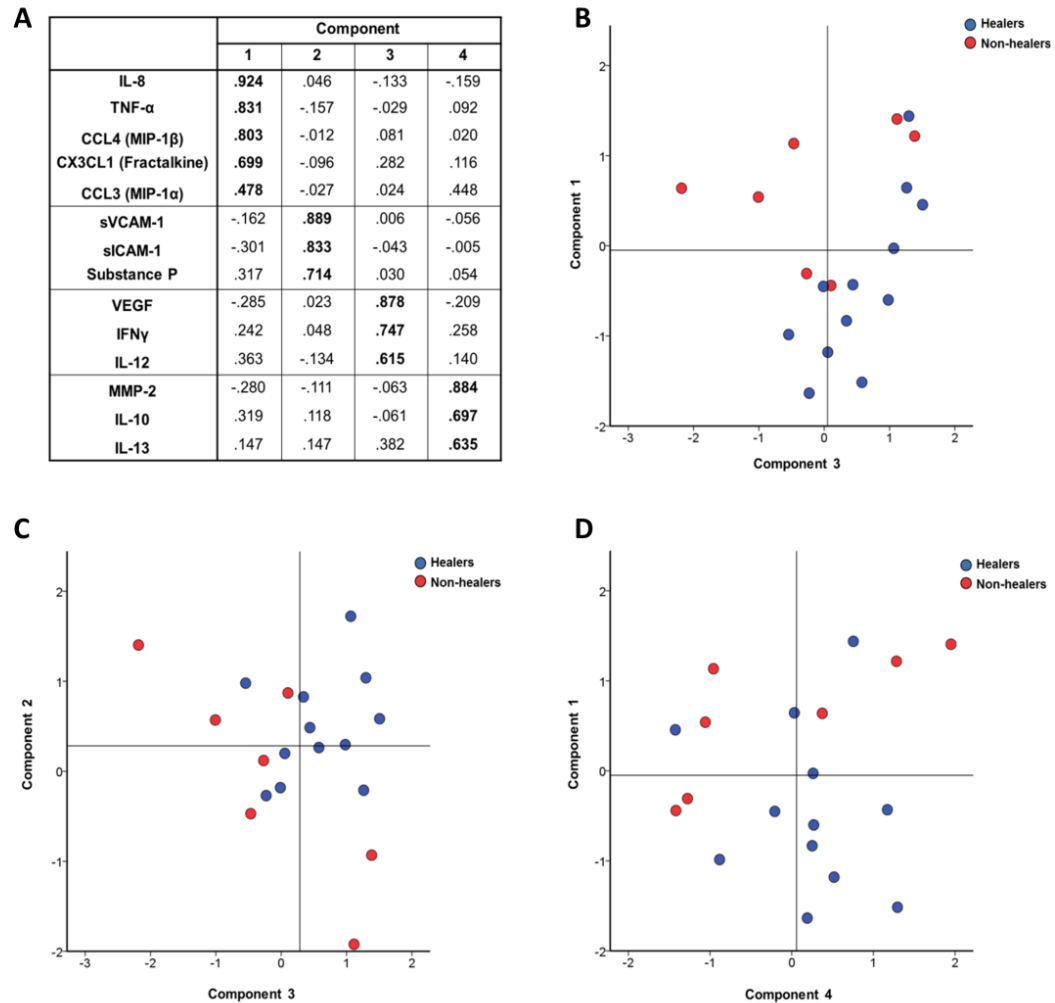


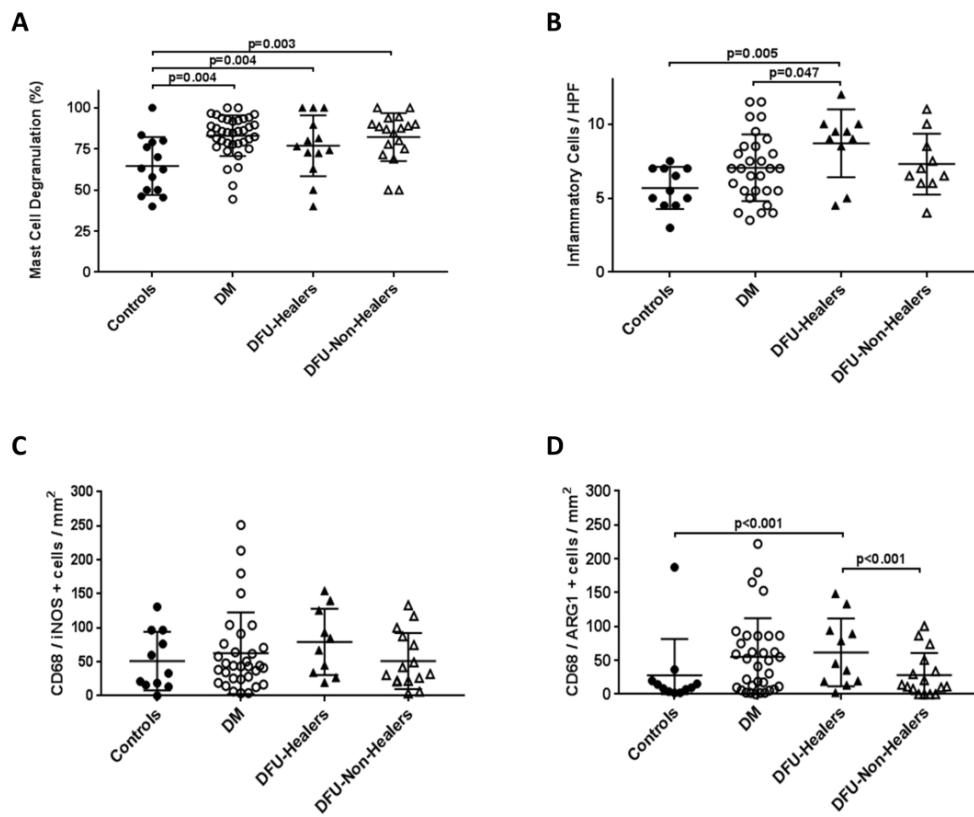
Supplemental Material

scRNA-Seq transcriptome analysis pipeline: The Cell Ranger Software Suite version 1.3 was used to perform sample demultiplexing, barcode processing and single-cell gene counting. The generated gene-cell-barcode matrices were subsequently loaded into R and analyzed with Seurat version 2.3.4 as detailed in the online Guided Clustering Tutorial (<https://satijalab.org/seurat/>). The filtered output from Cell Ranger was imported into a "Seurat object" for all samples belonging to each of the sample groups (DM, DFU and non-DM) separately, followed by QC analysis. The following filters were applied to each of the datasets on a per cell basis: maximum number of genes = 2000, minimum number of genes = 200, maximum number of UMIs = 6000, minimum number of UMIs = 200, maximum percentage of mitochondrial transcript abundance = 0.2. After filtering, each of the 3 objects was normalized using the log normalization method and a scaling factor of 10,000. The top 2,000 highly variant genes were then identified. To detect genes enriched in each cluster we utilized the Seurat function *FindAllMarkers()* with the default Wilcoxon rank sum test and 0.25 log fold change threshold for genes present in a minimum fraction of 25% of the cluster cells. Visualizations of data were done using Seurat and dittoSeq (<https://github.com/dtm2451/dittoSeq>).

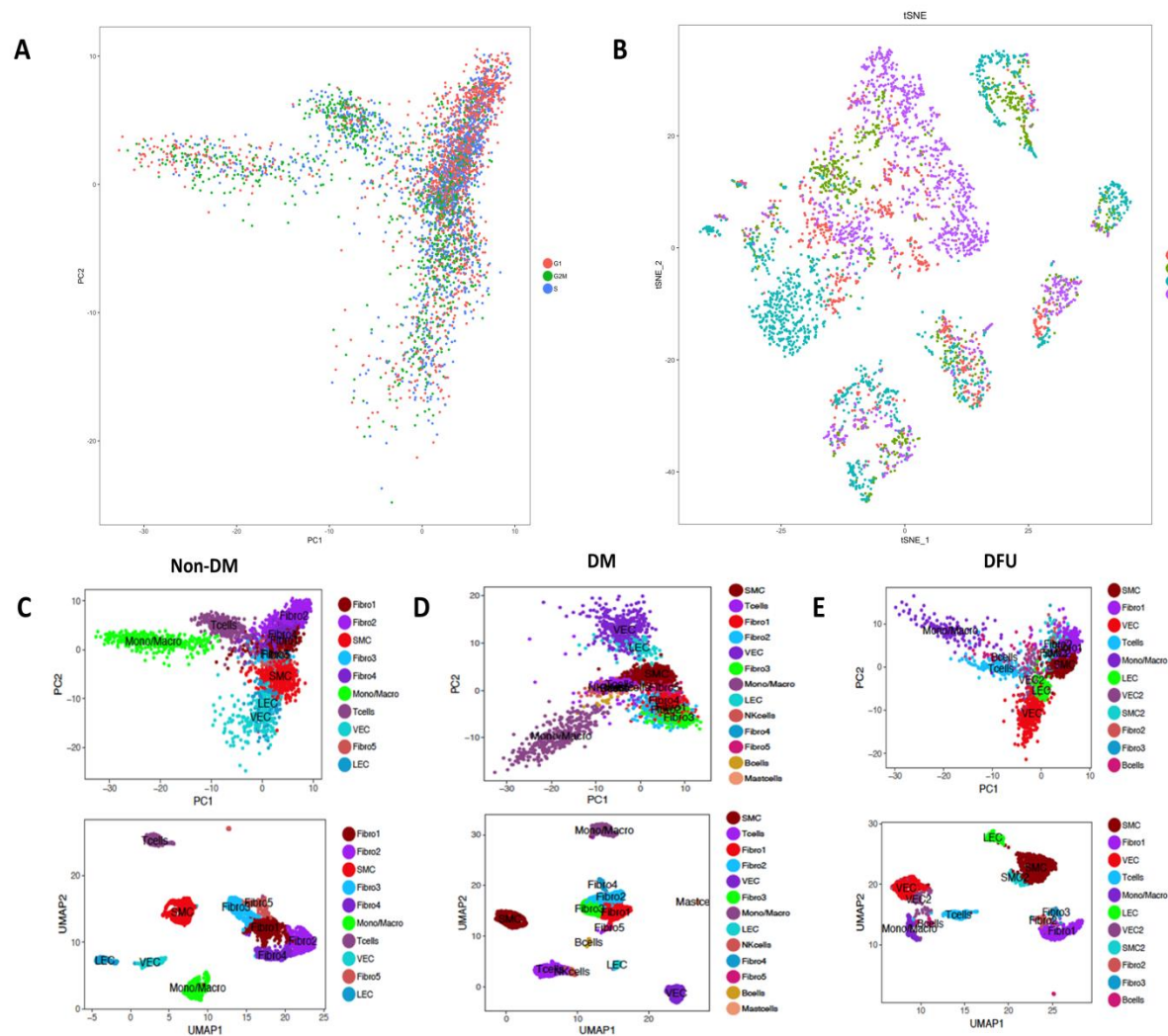
Supplementary Figure 1. Principal component analysis including serum inflammatory cytokines and chemokines, growth factors, and biomarkers of endothelial function at baseline performed with direct oblimin rotation. (A) Table representing the 4 principal components and loading for each variable. A loading >0.4 was considered significant. **(B-D)** Component scores for Healers (blue dots) and Non-Healers (red dots) at baseline. Vertical line represents the median. $n=7-12$ subjects; patients for whom there was at least one missing data point were not included in analysis.



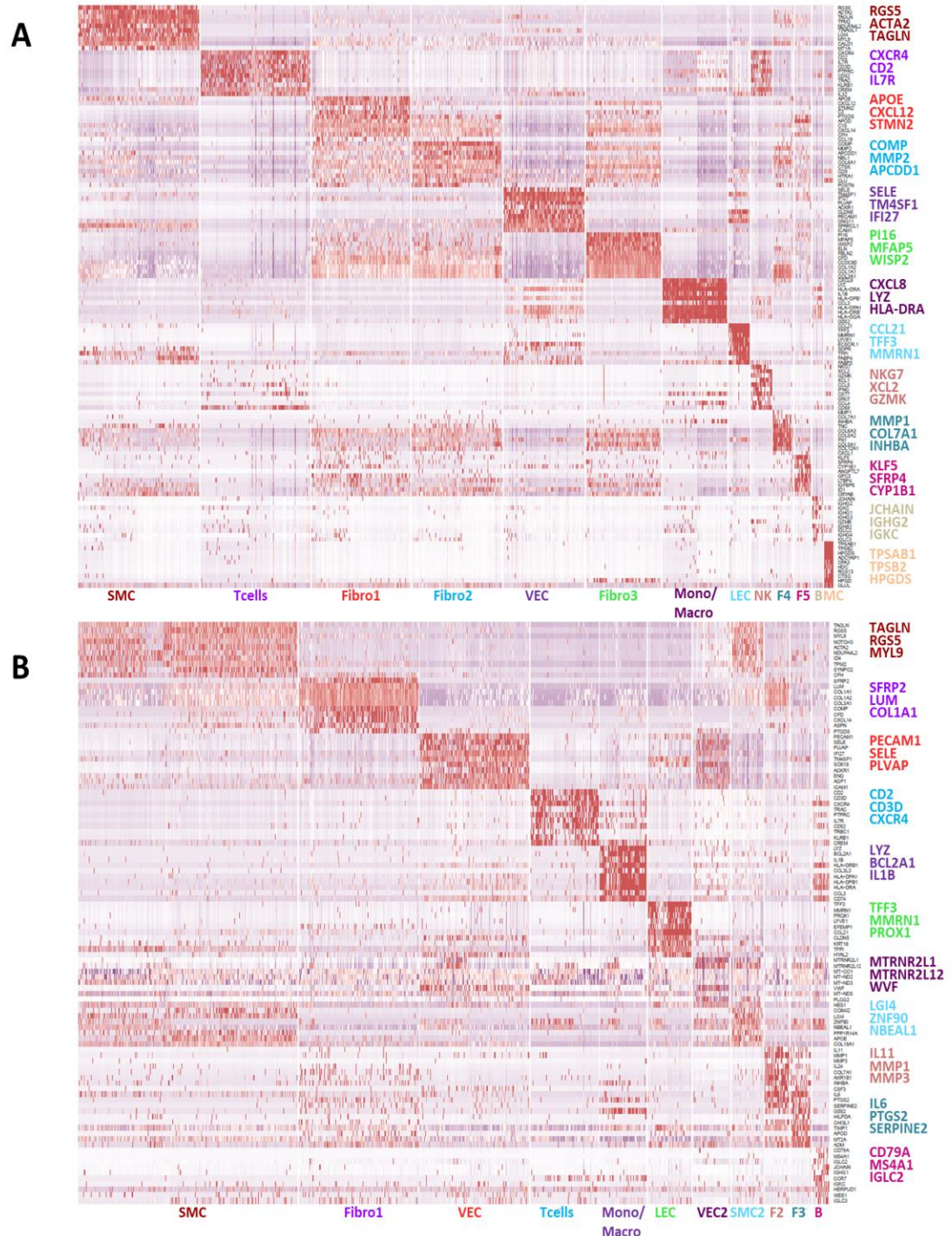
Supplementary Figure 2. Forearm biopsies' inflammatory cell profile (A) Diabetic (DM) patients with or without diabetic foot ulcer (DFU) display increased levels of mast cell degranulation % in forearm biopsies as measured from Toluidine Blue staining, n=13-37 subjects. (B) DFU patients who healed their ulcers (DFU-Healers) had more inflammatory cells per high-power field (HPF) in H&E stained forearm biopsies, n=10-29 subjects. (C) No differences were found in M1 associated macrophage marker staining; quantification of immunofluorescently stained CD68 and inducible nitric oxide synthase (iNOS) double positive cells in forearm biopsies, n=10-32 subjects. (D) DFU-Healers exhibited greater numbers of M2 associated macrophages as indicated by quantification of immunofluorescently stained CD68 and Arginase-1 (ARG1) double positive cells in forearm biopsies, n=11-33 subjects. Data are represented as mean \pm SD, statistically significant comparisons are displayed and calculated with one-way ANOVA with Fisher's *post-hoc* test.



Supplementary Figure 4. Cell cycle and different subjects' impact on cell clustering. We explored whether cell cycle was a major source of variation in our data by visualizing a PCA plot and coloring by cell cycle phase (G1, G2M, S) of each cell after the individual cells were scored according to a list of genes associated with specific cell phases utilizing the *AddModuleScore()* Seurat function. Cell cycle phase clusters superimpose by PCA (red:G1, green:G2M, blue:S) (A), indicating that cell phase was not a source of variation. Primary sources of heterogeneity were identified using principal component (PC) analysis and significant PCs (metagenes) were determined for clustering analysis. To select PC number, we plotted a scree plot and calculated where the PCs begin to “elbow” by obtaining the larger value of the point where the PCs contribute only 5% or less of the standard deviation, or the point where the PCs cumulatively contribute 90% of the standard deviation. This resulted in 16, 13 and 17 PCs for the healthy controls, DFU and DM groups, respectively. The PCs were then used for t-SNE dimensional reduction and visualization (using 0.8 resolution), and for clustering. Cells from each subject were indicated by Non-DM patients t-SNE plot colored by the four individual samples (red, green, blue, purple dots) depicting clusters largely including cells from all subjects (B). PCA (top) and UMAP (bottom) visualization plots for non-DM (C), DM (D) and DFU (E) subjects.

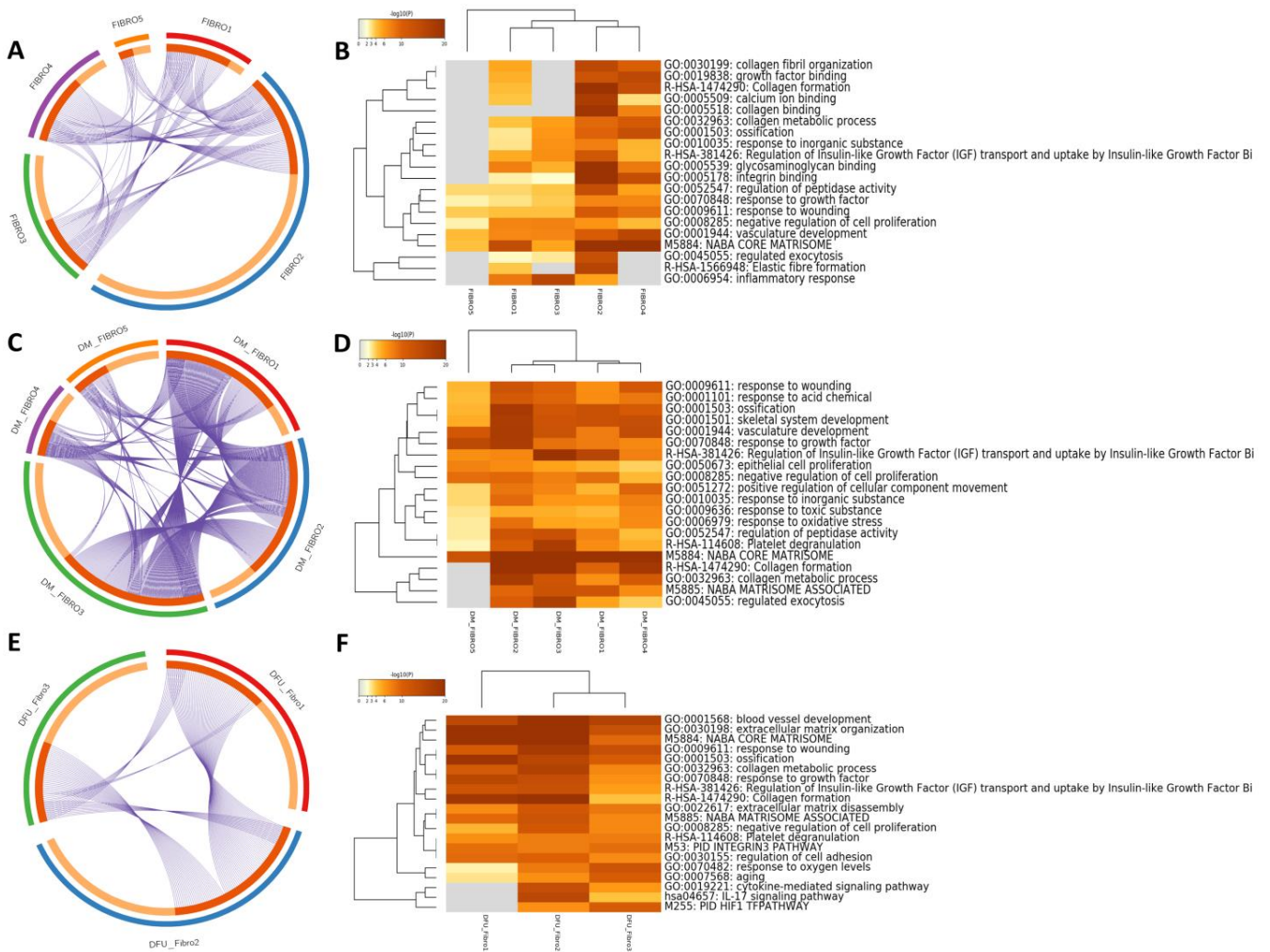


Supplementary Figure 5. Characterization of clustering analysis efficiency. Heatmap depicting distinct clusters and their top 10 (with top 3 highlighted) differentially expressed genes for DM (A) and DFU (B) conditions. Each column represents a single cell and each row represents an individual gene. Red corresponds to maximum relative gene expression. The colors for highlighted genes correspond to the colors of the respective cluster. F:Fibro, B:B cells, MC: Mast Cells.

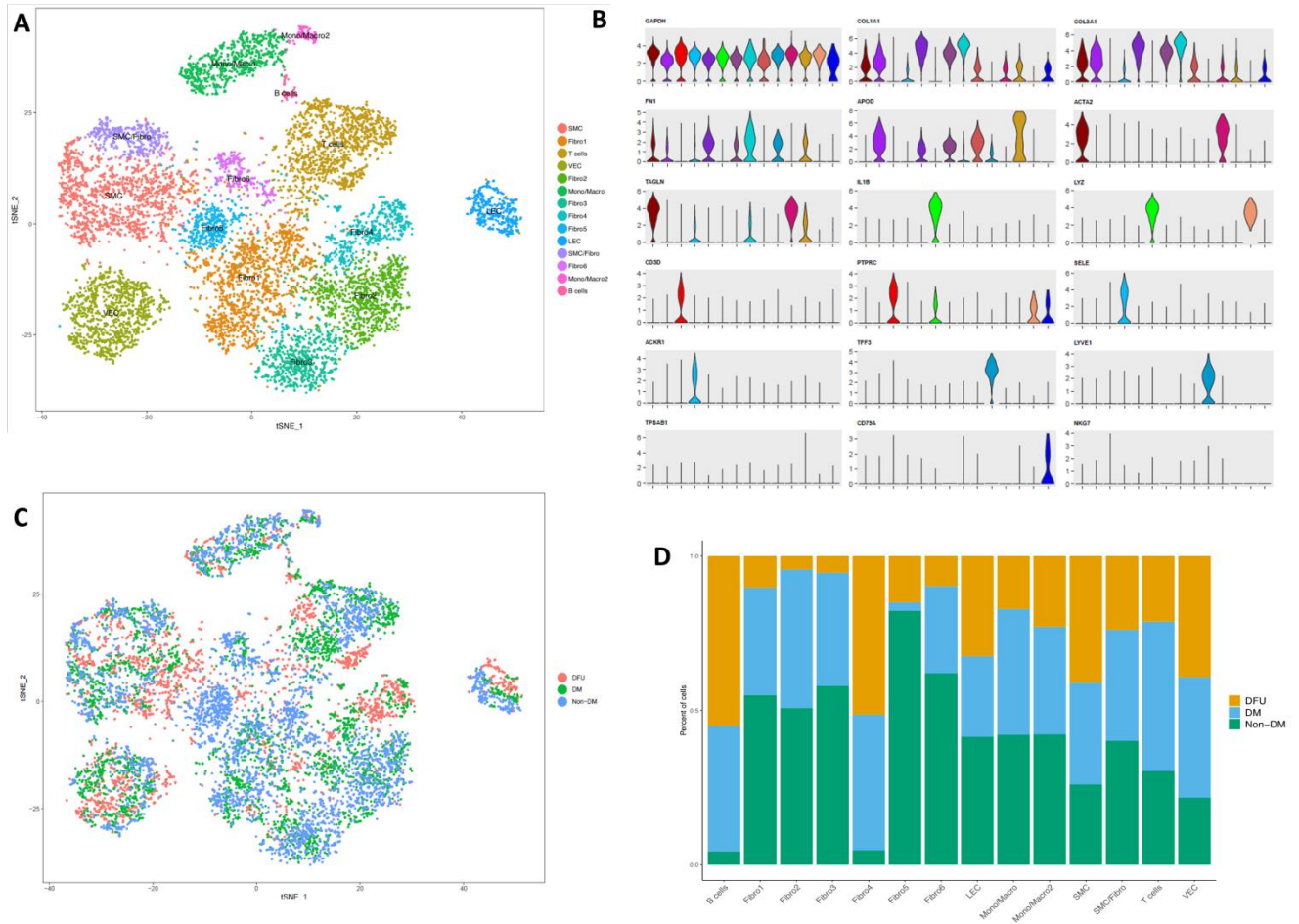


Supplementary Figure 6. Exploring fibroblast heterogeneity across different conditions. (A,C,E)

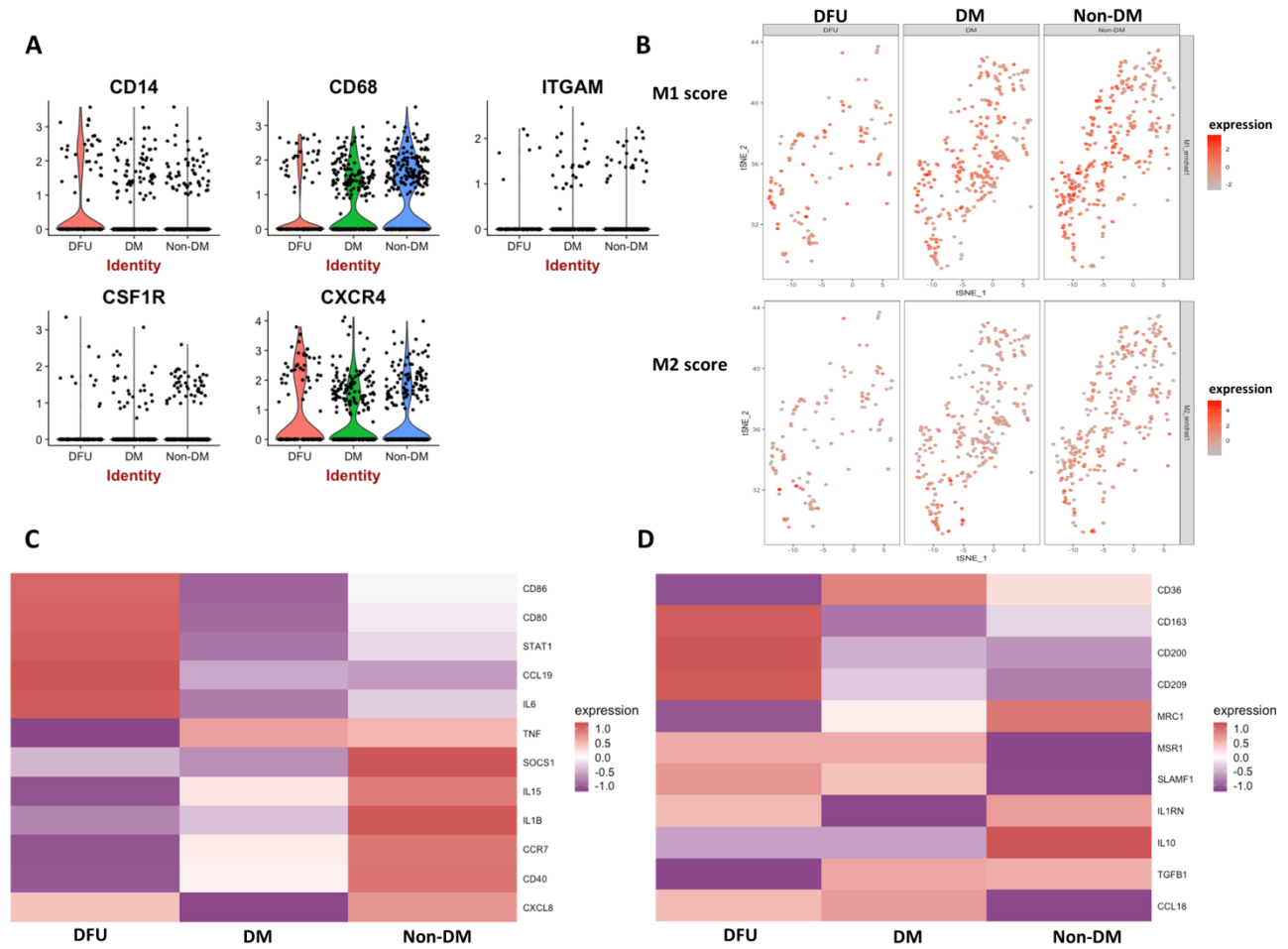
Circos diagrams showing overlap in differentially expressed genes across fibroblast enriched clusters in non-DM (A), DM (C) and DFU (E). Different clusters of fibroblasts are labelled and shown in different colors (Fibro1 red, Fibro2 blue, Fibro3 green, Fibro4 purple and Fibro5 orange). (B,D,F) Heat maps of enriched gene ontology (GO) terms in fibroblast clusters, colored by p -values (legend). Each column represents a different fibroblast cluster and each row an ontology term. Pathway and process enrichment analysis was performed using the following ontology sources: Kyoto Encyclopedia of Genes and Genomes (KEGG; Release 87.0), Gene Ontology (GO) Biological Processes (Version 2018-08-09) Molecular Signatures Database (Version 6.2) Reactome Gene Sets (Version 64) and CORUM (Version 3.0). All genes in the genome were used as the enrichment background. In the gene set enrichment analysis, p -values were calculated based on cumulative hypergeometric distribution and Q -values were calculated using the Benjamini-Hochberg procedure for multiple testing. A term was considered overrepresented when $p < 0.05$. To reduce redundancy in ontology terms, the terms with $p < 0.01$, a minimum count of 3 and an enrichment factor > 1.5 , which is the ratio between the observed counts and the counts expected by chance, were collected and grouped into clusters based on their membership similarities. In the process of hierarchical clustering of the enriched terms, k scores were used as the similarity metric, and sub-trees with similarity > 0.3 were considered to be a cluster. The most statistically significant term within a cluster was chosen to represent the cluster. All analyses were carried out using the web-based tool, Metascape (Version 3.0, <http://metascape.org>)



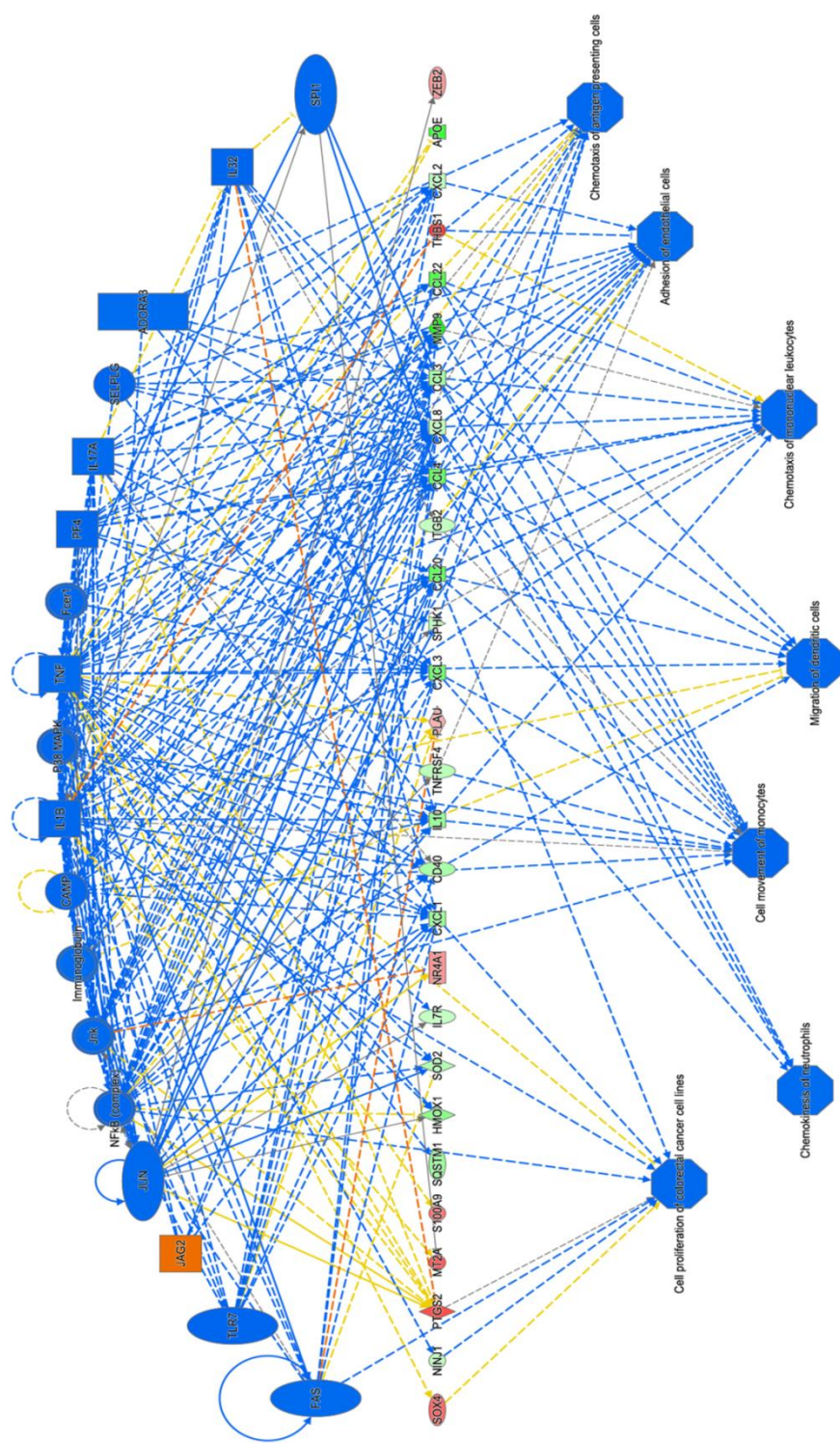
Supplementary Figure 7. Canonical Correlation Analysis (CCA) combining all scRNA-seq samples. Using the list of the top 500 genes with the highest dispersion, 20 canonical vectors were calculated. The ratio of variance explained by PCA was then calculated and data was subsetted based on the ratio (lowest accepted value was 0.5). The subspaces within each of the three objects were then aligned using the CCA reduction type, and all 20 dimensions calculated above were used for this step. Clusters were identified using the 20 dimensions and a resolution of 0.8. **(A)** Two dimensional plot derived in Seurat from t-SNE analysis of the single cell transcriptomes of all 9,878 cells from the foot skin of all 12 subjects. **(B)** Violin plots for different marker genes enriched in specific clusters. *GAPDH*, *FN1*, *TAGLN*, *CD3D*, *ACKR1*, *TPSAB1* (top to bottom left); *COL1A1*, *APOD*, *IL1B*, *PTPRC*, *TFF3*, *CD79A* (top to bottom middle); *COL3A1*, *ACTA2*, *LYZ*, *SELE*, *LYVE1*, *NKG7* (top to bottom right). **(C)** t-SNE plot with cells annotated per different conditions (DFU in red, DM in green and Non-DM in blue). **(D)** Stacked barplots show the proportion of cell types belonging to each cluster as listed on the x-axis per condition (orange for DFU, blue for DM and green for non-DM).



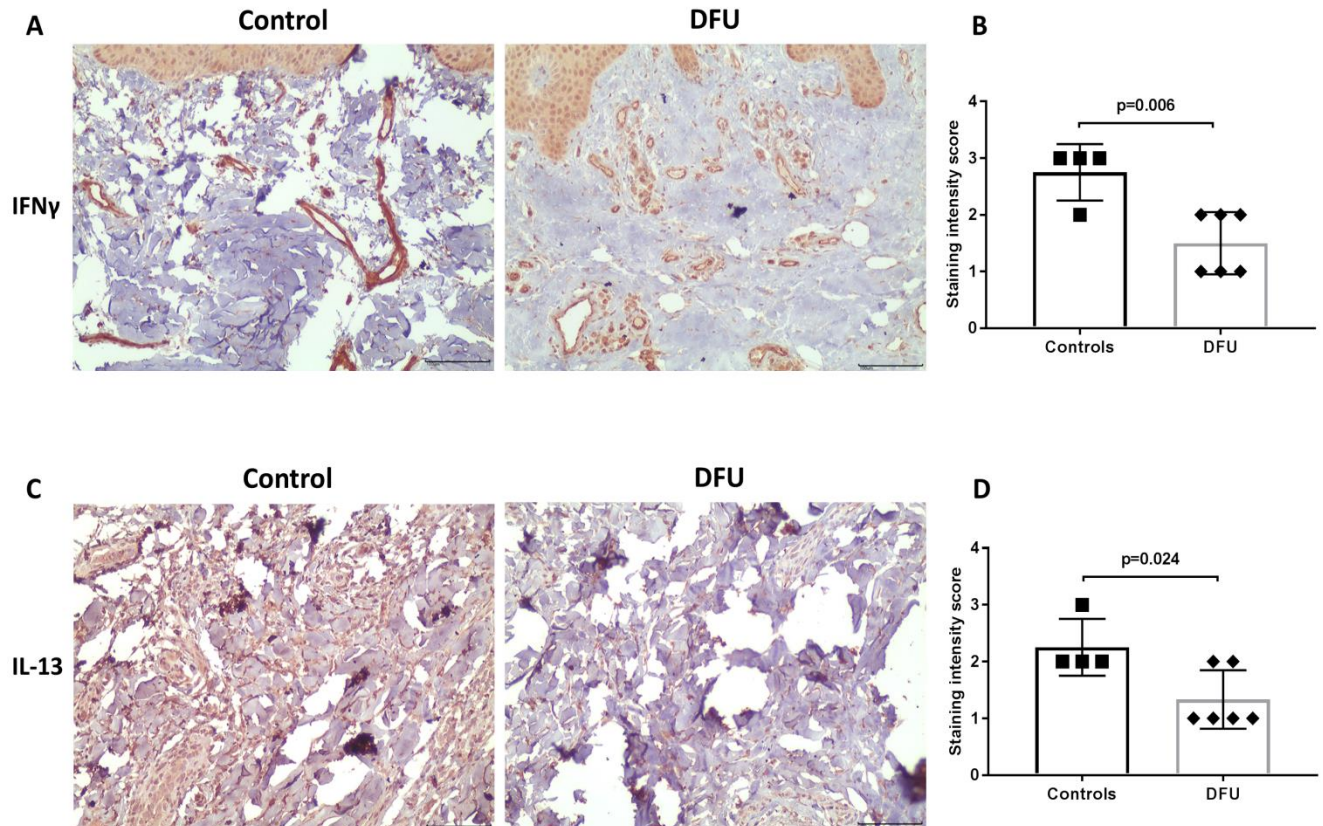
Supplementary Figure 8. Exploring the myeloid scRNA-seq cells cluster. (A) Violin plots for the expression of monocyte and macrophage markers across different conditions, dots indicate single cell and shape of violin correlates with expression distribution pattern. (B) M1(top) and M2 (bottom) enrichment scores across the different conditions. Intensity of red color correlates with higher scores. (C) Selected M1 associated marker genes (*CD86*, *CD80*, *STAT1*, *CCL19*, *IL6*, *TNF*, *SOCs1*, *IL15*, *IL1B*, *CCR7*, *CD40*, *CXCL8* top to bottom) expression in myeloid cells cluster, per condition (DFU, DM, non-DM). (D) Selected M2 associated marker genes (*CD36*, *CD163*, *CD200*, *CD209*, *MRC1*, *MSR1*, *SLAMF1*, *IL1RN*, *IL10*, *TGFB1*, *CCL18* top to bottom) expression in myeloid cells cluster, per condition (DFU, DM, non-DM). Red denotes high and purple low expression and intensity of color correlates with levels of expression.



Supplementary Figure 9. DM vs Non-DM combined analysis for upstream regulators and regulator effects in myeloid cell cluster. 17 upstream regulators located at the top of the network were predicted to be inhibited, all with the exception of one, which was activated. These regulators include IL1B, NFKb complex, IL17A, TLR7 and IL32. They in turn drive the expression changes of the genes in the middle tier comprising among others MMP9, CD40, IL10 and CCL4 and may lead to the inhibition of the biological processes listed at the bottom of the network and include chemokinesis of neutrophils, cell movement of monocytes, migration of dendritic cells and chemotaxis of antigen presenting cells.



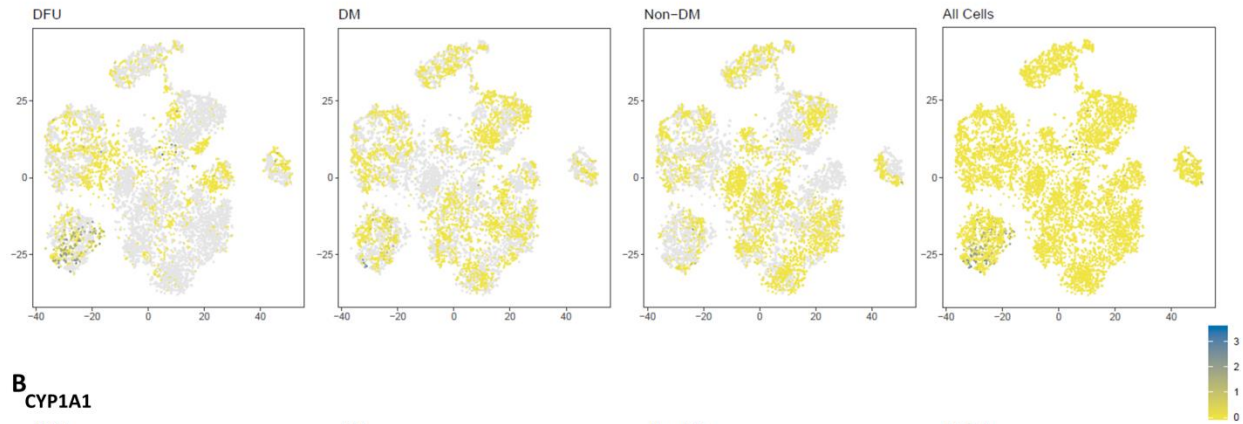
Supplementary Figure 10. Protein validation of transcriptional regulators. Representative micrographs of immunohistochemically stained foot skin tissue from controls and diabetic ulcers (DFU) reveal reduced expression of interferon gamma (IFN γ) (A,B) and interleukin 13 (IL-13) (C,D) in DFU. Both cytokines were widely expressed in different cell types, notably around blood vessels. Quantification was performed by an experienced dermatopathologist (A.K.) blindly scoring on a scale of 1 (lowest) to 3 (highest) expression, n=4-6 subjects. Data are represented as mean \pm SD, statistically significant comparisons are displayed and calculated with unpaired *t*-test. Scale bars = 100 μ m.



Supplementary Figure 11. Differentially expressed genes from forearm skin non-healers bulk RNA-seq at single cell level. t-SNE plots of Prostaglandin transporter (*SLCO2A1*) (A) and Cytochrome P450, family 1, subfamily A, polypeptide 1 (*CYP1A1*) (B) expression across the different conditions (DFU, DM, Non-DM left to right). Each dot represents one cell with yellow denoting no and green denoting high expression and intensity of color corresponding to increased expression levels, according to the scale on the right. All the cells are also shown together in the same plot (far right).

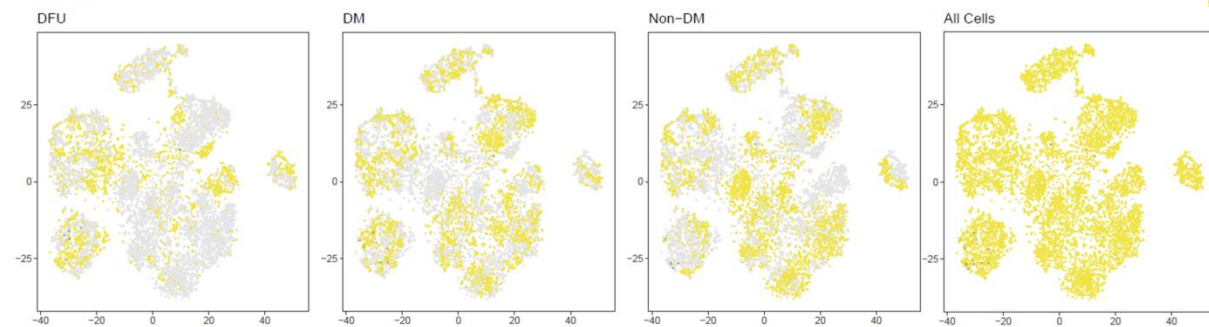
A

SLCO2A1



B

CYP1A1



Supplementary Table 1. List of antibodies used in this study.

Antibody	Clone	Manufacturer	Dilution
Mast cell tryptase	AA1	Abcam; ab2378	1:150
IFN- γ	G-23	Santa Cruz Biotechnology; sc-8423	1:50
IL-13	Polyclonal	Abcam; ab106732	1:100
CD68	EPR20545	Abcam; ab213363	1:50
HLA-DR	TAL 1B5	Abcam; ab20181	1:100
iNOS	NOS-3F7-B11 B5	ThermoFisher; MA3-030	1:100
CD206	D-1	Santa Cruz Biotechnology; sc-376108	1:100
ARG1	N-20	Santa Cruz Biotechnology; sc-18351	1:100

Supplementary Table 2. Comparisons of cytokines, growth factors and biomarkers of endothelial function at baseline visit.

	Controls	DM	Healers	Non-Healers	P value
Macrophages (CD68)	14 (4-51)	22 (12-37)	28 (8-56)	28 (14-35)	0.79
M1 (iNOS-CD68)	33 (16-97)	44 (25-75)	76 (32-129)	32 (22-88)	0.75
M2 (ARG1-CD68)	10 (4-20)	50 (9-86)	45 (19-94)*	13 (2-47) ‡	0.059
MMP-2 (ng/mL)	199 (185-224)	202 (159-242)	193 (143-223)	182 (146-263)	0.79
MMP-9 (ng/mL)	128 (99-157)	102 (73-170)	131 (72-173)	111 (79-157)	0.82
sICAM (ng/mL)	103 (83-131)	112 (98-135)	139 (107-177)	103 (79-144)	0.06
sVCAM (ng/mL)	540 (395-652)	534 (424-647)	739 (457-867)	434 (279-697)†‡	0.01
ITAC (pg/mL)	14.0 (7.2-23.3)	16.4 (8.7-27.1)	18.4 (7.1-37.2)	23.3 (14.5-38.9)	0.3
GM-CSF (pg/mL)	20.5 (13.4-30.9)	14.6 (6.9-37.4)	24.1 (11.3-36.0)	14.3 (6.9-38.6)	0.45
Fractalkine (pg/mL)	44.3 (32.0-57.0)	44.2 (29.7-73.4)	40.1 (27.2-85.2)	59.3 (25.4-140.8)	0.51
IFN γ (pg/mL)	18.9 (13.6-29.5)	14.3 (9.2-23.8)*	18.0 (12.3-22.7)	11.0 (6.8-26.1)*	0.03
IL-10 (pg/mL)	6.48 (3.01-12.48)	4.25 (1.84-8.78)	4.61 (2.49-11.90)	3.35 (1.38-7.61)	0.3

MIP-3 α (pg/mL)	13.9 (11.6-18.4)	11.4 (8.0-17.7)	10.9 (7.4-21.3)	11.0 (7.6-17.6)	0.3
IL-12 (pg/mL)	1.51 (0.98-2.24)	1.70 (1.05-3.35)	2.28 (0.93-3.26)	1.07 (0.72-2.81)	0.8
IL-13 (pg/mL)	5.60 (4.14-9.17)	5.26 (2.21-7.59)	3.87 (3.16-6.76)	2.80 (1.13-7.19)	0.18
IL-17a (pg/mL)	6.95 (3.49-13.47)	5.21 (2.20-8.67)	7.09 (2.34-10.51)	3.45 (1.62-7.79)	0.07
IL-1 β (pg/mL)	1.41 (0.92-2.50)	1.14 (0.53-2.49)	1.59 (1.01-2.22)	0.96 (0.47-2.40)	0.69
IL-2 (pg/mL)	2.47 (1.03-3.76)	1.65 (0.73-3.47)	2.35 (1.47-3.31)	1.33 (0.76-3.36)	0.71
IL-21 (pg/mL)	1.16 (0.56-1.79)	0.89 (0.30-2.93)	1.67 (0.40-2.52)	0.78 (0.25-1.24)	0.47
IL-4 (pg/mL)	14.0 (5.1-37.8)	8.3 (3.4-29.1)	14.3 (4.8-22.9)	13.8 (3.0-38.4)	0.3
IL-23 (pg/mL)	39.1 (24.2-129.9)	40.9 (19.0-130.8)	81.7 (32.0-114.7)	44.9 (20.7-72.8)	0.71
IL-5 (pg/mL)	2.35 (0.70-4.17)	1.61 (1.03-2.98)	2.14 (1.01-3.12)	1.97 (0.73-3.72)	0.97
IL-6 (pg/mL)	2.38 (1.33-4.06)	1.60 (0.98-3.03)	2.51 (1.51-4.83)	2.79 (1.41-6.31) [†]	0.03
IL-7 (pg/mL)	11.7 (7.7-15.3)	8.6 (5.1-13.7)	10.9 (7.6-15.5)	6.1 (2.9-17.7)	0.19
IL-8 (pg/mL)	4.6 (3.4-6.5)	4.6 (2.8-6.0)	2.8 (2.5-7.6)	7.0 (4.2-9.9)	0.07
MIP-1 α (pg/mL)	12.0 (9.3-15.5)	10.5 (7.7-14.7)	9.8 (7.4-11.9)	10.2 (7.5-20.5)	0.72
MIP-1 β (pg/mL)	12.0 (9.4-16.4)	11.1 (8.7-17.1)	11.0 (10.0-15.4)	15.3 (9.7-24.7)	0.44
TNF α (pg/mL)	6.4 (4.7-8.3)	4.3 (3.2-6.4)*	4.9 (4.0-8.5)	8.2 (4.8-10.7) ^{†‡}	0.001
EGF (pg/mL)	85 (58-97)	60 (36-144)	61 (20-89)	69 (35-112)	0.31
FGF2 (pg/mL)	219 (81-501)	185 (90-390)	166 (50-354)	137 (70-268)	0.5
VEGF (pg/mL)	705 (397-1701)	658 (278-1180)	789 (577-1729)	298 (102-914) * ^{†‡}	0.01
Substance P (pg/ml)	545 (255-624)	461 (400-620)	492 (429-665)	456 (377-588)	0.41

Data are expressed as median (interquartile range). Comparison were made using ANOVA and LSD post-hoc test on log transformed data. * vs controls; [†] vs DM; [‡] vs DFU Healers.

Supplementary Table 3. Measures of lower extremity skin microvascular function. The vascular reactivity of the foot skin microcirculation was evaluated by Laser Doppler perfusion imaging measurements before and after the iontophoresis of acetylcholine chloride (ACh, endothelium-dependent vasodilation) and sodium nitroprusside (SNP, endothelium-independent vasodilation). The flow mediated brachial artery dilation (FMD, endothelium dependent) and nitroglycerine-induced dilation (NID, endothelium independent) were measured in accordance with published guidelines.

	Controls	DM	Healers	Non-Healers	P-value
ACh iontophoresis					
Baseline	9.9 (7.0-15.2)	7.8 (5.1-16.9)	13.1 (5.7-18.3)	15.8 (7.7-27.3)	0.16
% change from baseline	81.9 (29.4-296.0)	75.8 (16.1-209.5)	13.3 (2.5-105.6)	6.4 (1.3-59.6)* †	0.023
SNP iontophoresis					
Baseline	8.7 (4.5-13.6)	9.9 (5.3-19.8)	13.0 (8.1-34.7)	15.6 (6.9-42.5)	0.17
% change from baseline	48.5 (-1.4-148.2)	67.4 (21.0-142.2)	42.5 (-8.0-168.9)	39.8 (8.4-168.1)	0.82
FMD%	8.44 ± 1.97	7.32 ± 1.62*	5.94 ± 1.91*†	6.47 ± 1.81*†	<0.0001
NID%	18.73 ± 4.34	16.72 ± 4.96	12.36 ± 5.57*†	14.40 ± 5.62*	0.002

* vs controls; † vs DM;

Supplementary Table 4. Quantification of mast cell degranulation and inflammatory cells in forearm biopsies.

	Controls	DM	Healers	Non-Healers	P-value
Degranulated mast cells (toluidine blue, %)	62.8 (49.0-79.2)	85.0 (78.0-92.6)*	76.5 (67.7-94.7)*	87.2 (74.1-90.9)*	0.006
Degranulated mast cells (tryptase, %)	75.0 (42.0-90.0)	84.6 (71.0-96.1)	85.9 (60.4-100)	83.2 (71.9-100)	0.50
Total inflammatory cells (H&E staining)	5.5 (4.5-7.0)	7.0 (5.5-8.5)	9.3 (7.6-10.0) †*	6.8 (6.0-8.9)	0.03

*vs controls; † vs DM.

Supplementary Table 5. Bulk RNA-seq samples details.

Age, years	Sex	Condition	RIN
57	M	DM	7.2
61	M	DM	7.6
61	M	DM	7
60	M	DM	8
59	M	Healer	8.2
65	M	Healer	7.3
61	M	Healer	8.7
50	M	Healer	7.8
52	F	Healer	8.1
55	M	Non-Healer	7.2
53	M	Non-Healer	7.9
55	M	Non-Healer	8.1
53	F	Non-Healer	8.4

Supplementary Tables 6, 7 and 8: <https://figshare.com/s/3ce46837ac076caa2c49>

Supplementary Table 9. Patient demographics and surgery details for single cell RNA sequencing experiments including ulcer size.

Patient	Age, years	Sex	Condition	Type of Surgery
1	75	F	Non-DM	Left foot 2nd digit bunionectomy
2	58	F	Non-DM	Bilateral 2nd & 4th hammertoe correction
3	56	F	Non-DM	Left foot lapidus bunionectomy
4	60	F	DFU	Surgical excision ulcer left foot; 1.5 x 2 cm
5	44	M	DM	Fusion interphalangeal joint right
6	49	F	DFU	Surgical excision ulcer right foot; 1x1 cm
7	49	F	DM	Excision of plantar foot fibroma
8	53	F	DM	Metatarsal cuneiform fusion
9	63	F	Non-DM	Left foot bunionectomy
10	65	F	DM	Excision spur right foot 5th toe
11	66	M	DFU	Surgical excision ulcer 2nd digit left foot; 0.75x0.5 cm
12	60	M	DFU	Surgical excision ulcer right foot; 0.5x0.5

				cm
--	--	--	--	----

Supplementary Tables 10, 11, 12 and 13: <https://figshare.com/s/5ba30d82331e68619f3c>

Supplementary Table 14. List of M1 (60 genes) and M2 (52 genes) macrophage phenotype associated markers utilized for scoring the myeloid cell cluster in the sc-RNA-seq dataset.

M1-associated genes	M2-associated genes
CD86	CD163
CD80	THBS1
CD64	CCL17
SOCS1	CD1A
IDO	CD1B
IFNG	CCL22
CCR7	TGM2
IL12RA	FCER2
IL15RA	MRC1
IL7R	MS4A4A
CXCL11	CD36
CCL19	MS4A6A
CXCL10	CLECSF13
CXCL9	DCSIGN
TNF	P2RY14
CCL5	DECTIN1
CCL15	CXCR4
IL12B	MSR1
IL15	DCL1
TRAIL	TLR5
IL6	HRH1
CCL20	TGFBR2
PBEF1	P2RY5
ECGF1	GPR86
BCL2A1	CCL13
FAS	CCL18
BIRC3	CCL23
GADD45G	IGF1

HSXIAPAF1	SLC38A6
SLC7A5	SLC4A7
SLC21A15	SLC21A9
SLC2A6	HS3ST1
SLC31A2	ALOX15
INDO	CA2
PLA1A	LTA4H
OASL	HS3ST2
CHI3L2	CERK
HSD11B1	TPST2
AK3	HNMT
SPHK1	ADK
PFKFB3	LIPA
PSME2	HEXB
PFKP	CTSC
PSMB9	FGL2
PSMA2	FN1
OAS2	CHN2
PTX3	SEPP1
CSPG2	TGFBI
APOL3	MAF
IGFBP4	EGR2
APOL1	GAS7
PDGFA	
EDN1	
APOL2	
INHBA	
APOL6	
HESX1	
IRF1	
ATF3	
IRF7	